SUITMA+20

Water and thermal regime of extensive green roof test beds planted with sedum cuttings and sedum carpets

Michal Sněhota[1,2] · Jitka Hanzlíková[1,2] · Martina Sobotková[1] · Philip Moravcik[3]

Abstract

Purpose Implementation of green roofs could help to reduce rapid runoff and help cities to mitigate heat islands. The aim of the study is to assess the water and temperature regimes of four experimental green roof test beds having different growing media and plant coverage during the vegetation season 2018.

Materials and methods Experiments were conducted in four test beds (1 × 1 m) established on a flat roof. Two types of growing media were used. The first (A) was a substrate composed of crushed spongolite, crushed expanded clay, and peat. The second (B) was a coarser substrate, composed of crushed expanded clay, crushed bricks, peat, and compost. Two test beds, hereafter designated ACu and BCu, were filled with substrates A and B respectively and planted with a mixture of *Sedum* spp. cuttings with approximately 10% coverage. The substrate thickness was 6 cm. Two other test beds, designated ACa and BCa, were filled to a depth of 4 cm with A and B growing media, respectively, and planted with a carpet of *Sedum* spp. with approximate coverage of 100%.

Results and discussion The experiment was conducted over one growing season. Continuous monitoring of substrate temperature, water content, and outflow was conducted on each test bed. The lowest runoff coefficient was observed in test bed ACu, while the highest runoff occurred in test bed BCu, with twice the amount of outflow as ACu. The total runoff coefficient of ACa was more than one-third higher than that of ACu. The lowest maximum substrate temperature on the hottest day of the season was observed in bed ACa with a temperature of 40.6 °C, while the highest temperature was seen in bed BCu, 7.9 °C higher.

Conclusions The analysis of the rainfall-runoff relationship calculated for individual rainfall events demonstrated that runoff coefficients depended on initial water content, rainfall intensity, rainfall depth, substrate type, and vegetation cover. Beds planted with sedum carpets and having more extensive vegetation coverage were superior at moderating extremes of temperature.

Keywords Extensive green roof · Substrate · Water regime · Thermal regime · Water retention · Constructed soil

✉ Michal Sněhota
   michal.snehota@cvut.cz

1   Faculty of Civil Engineering, Czech Technical University in Prague, Thákurova 7, Prague 6, 166 29 Prague, Czech Republic

2   University Centre for Energy Efficient Buildings, Czech Technical University in Prague, Třinecká 1024, Buštehrad, 273 43 Buštehrad, Czech Republic

3   Water Resources Research Center, University of Hawaii at Manoa, 2540 Dole St., Holmes Hall 283, Honolulu, HI 96822, USA

1 Introduction

Architects and designers are increasingly employing green roofs to reduce the impacts of climate change in the built environment. These impacts include temperature extremes and accelerated runoff (Lehmann 2014). These phenomena have been observed more frequently in recent years. Temperature extremes have direct public health significance. Robine et al. (2008) determined that there were 70,000 additional deaths in Europe caused by the heatwave of 2003. Urban heat islands can be mitigated through evapotranspiration occurring on green roofs (Bevilacqua et al. 2016) which represent a relatively low-cost, low-tech design feature that can be incorporated into new construction or retrofitted on existing buildings. Retrofitting can be accomplished quickly as a timely response to the rapid increases in summer temperatures and extreme rainfall events that are occurring. Putting

green roofs on impervious roofs can reduce the health impacts and the excess burden placed on the power grid and drainage systems caused by these increases.

A less publicized, but arguably equally important, benefit of green roofs is their capacity to delay and reduce runoff from impervious roofing materials. Rapid runoff from hardened surfaces is associated with a variety of problems including flooding, erosion, overwhelmed drainage infrastructure, and the transport of pollutants to natural waters (Mentens et al. 2006).

Previous research into the performance of green roofs includes many studies comparing hydrological and thermal properties of different substrates with similar vegetation cover, or similar substrates with different plant species. Notable investigations into runoff reductions from large scale green roofs include (Akther et al. 2020; Bengtsson et al. 2005; Berndtsson et al. 2009; Versini et al. 2020) and small scale green roofs (Beecham and Razzaghmanesh 2015; Brandao et al. 2017; da Silva et al. 2020; Gong et al. 2019; Skala et al. 2020; Stovin 2010; VanWoert et al. 2005; Wang et al. 2017; Voyde et al. 2010). These previous studies have found that the key parameters that determine runoff quantity from green roofs are slope and substrate depth (Sun et al. 2014; Speak et al. 2013; Van Woert et al. 2005), as well as physical properties of the substrate, rainfall intensity, initial water content, and degree of coverage (Li et al. 2018; Schroll et al. 2011).

The water retention capacity of green roofs also depends on vegetation coverage and vegetation type. Schroll et al. (2011) demonstrated significantly higher water retention on a vegetated roof compared with a roof covered with the same substrate but without vegetation. At the level of individual rainfall events, this effect depended strongly on the rainfall depth. The difference in water retention was observed only during the summer months because of the plants' transpiration. Berretta et al. (2014) conducted a study in Sheffield, UK, comparing the retention capacity of a sedum carpet-based test bed with that of a meadow-flower test bed on two commercial substrates. They found that the sedum test bed displayed greater retention. Li et al. (2018) showed that succulent plants (such as sedums), unlike grasses, did not significantly contribute to interception at the leaf level during any season of the year. The results of their study showed that reduction of runoff by green roofs with succulents was mainly due to evapotranspiration rather than by interception by the plants.

There is still a very limited amount of literature focused on performance of green roofs planted with sedum carpets. Sedum carpets generally consist of *Sedum* spp. plants pre-grown on coconut mats covered with a thin substrate layer. No study was found that compared in detail the hydrologic performance of two different substrates combined with two different planting methods, especially when sedum carpets were used.

This study focused on evaluating the hydrologic (runoff reduction and delay) and thermal regulating performance of specific combinations of two different substrates (coarser and finer) with two different planting methods. The research should provide the missing data on the degree to which rainfall retention differs under identical weather conditions for coarser and finer substrates with partial, and nearly complete vegetation cover.

2 Materials and methods

2.1 Site characterization

The current study utilized four raised beds previously established on the roof of the University Centre for Energy Efficient Buildings (UCEEB) in Buštehrad, Czech Republic (50° 9.41797′ N, 14° 10.19195′ E, 355 m a.s.l.) (described in detail by Jelinkova et al. (2015) and Jelinkova et al. (2016). Figure 1 shows the location of the experimental setup on the roof. The site is listed as a case study in a comparison of nature-based solutions by Bouzouidja et al. (2020 in this issue). The site region is characterized as temperate, with an average annual rainfall between 500 and 550 mm, and average air temperature of 8 °C. (long-term average in the period 1981–2010, Czech Hydrometeorological Institute).

During the course of our study, a weather station adjacent to the experimental site monitored the air temperature at heights of 7 and 200 cm, relative humidity, rainfall intensity, wind speed and direction, and net radiation. The weather observations were processed every 10 s and recorded as 1-min averages. Rainfall was monitored by a rain gauge as 1-min totals.

Weather conditions during the period are presented in electronic supplementary material S3. The average air temperature at 2 m above the roof surface during the monitoring period was 16.9 °C, the maximum air temperature reached 35.7 °C, and the minimum air temperature was 0.0 °C. The total rainfall depth was 249 mm, where June was the rainiest month with a rainfall depth of 81.2 mm. The prevailing wind direction during the study period was south-west. The 2018 growing period was significantly dryer than the long-term average in the region.

2.2 Green roof test beds

Two types of lightweight green roof substrate were used to construct four test beds. The first substrate is a commercially available substrate intended for extensive green roofs (Acre, Ltd., Czech Republic) hereafter referred to as substrate A. It is composed of crushed expanded clay, peat, and crushed natural spongolite, with other minor components. The composition provides sufficient capacity to collect and retain water while

Fig. 1 Experimental site of four raised beds established on the green roof at the University Centre of Energy Efficient Buildings, Czech Technical University in Prague

maintaining adequate permeability. The second substrate (B) is another commercially available extensive green roof substrate produced by BB Com Ltd., Czech Republic, composed of crushed expanded clay, crushed bricks, peat, and compost. The substrates have contrasting physical properties. Both are commonly used in the Czech Republic.

Test beds ACa (filled with A substrate, 4-cm depth) and BCa (filled with BBcom substrate, 4-cm depth) were planted with commercially available sedum carpet (Sedum Top Solution, Ltd., Czech Republic). The sedum carpet consisted of pre-grown vegetation on coconut mats (thickness from 2.5 to 4 cm) woven with a polypropylene mesh and containing a substrate layer with a mixture of vegetation. The mats were approximately 90% covered with vegetation. The sedum carpet included several *Sedum* species, especifically *S. sexangulare, S. album, S. Al.* "coral carpet," *S. lydium, S. lydium glauca, S. hispanicum minus, S. acre, S. reflexum, S. ref.* "Angelina," *S. spurium fuldagut, S. hybridum* "Immergrunchen," *S. kamtschaticum.* A photograph of the pre-cultivated sedum carpet is shown in Fig. S2 in Electronic supplementary material ES2.

Test bed ACu (filled with A substrate, 6 cm depth) and test bed BCu (BBcom substrate, 6-cm depth) were planted with a mixture of *Sedum* spp. cuttings. The sedum cuttings were collected from the sedum carpets to ensure the same species composition. Approximately 100 g of mixed sedum cuttings per square meter were used to plant the test beds. All four beds were planted in October 2017.

As can be seen in the aerial photograph—Fig. 2, the test beds were distributed in an area of 3 × 6 m, where the greatest distance between the test beds was 1 m and the shortest was approximately 0.5 m. There were no significant obstacles to rain, wind, and sunlight in the vicinity of the test beds. Datalogger boxes positioned east of the installation were low and did not cause significant shading except for a brief period early in the morning on certain days of the year. Under this arrangement, it is reasonable to assume that the test beds were exposed to identical weather conditions.

2.3 Substrate properties

2.3.1 Physical properties

The physical properties of the substrates were determined from samples collected during and after the installation of the test beds. Laboratory tests were carried out according to the Guidelines for the Planning, Construction and Maintenance of Green Roofing. (FLL 2008). Particle size distribution was determined by a combination of sieving and hydrometer methods (Casagrande 1934).

The particle size distribution of both green roof substrates (A and B) is shown in Table 1. Particle size distributions were determined on disturbed samples of the substrates from the test beds, by sieving and sedimentation methods. The B substrate had a greater percentage of coarse particles (12.5–2 mm). The coarser texture of the BB Com substrate corresponds to its lower water holding capacity. The A and B substrates were both texturally classified as sandy loam.
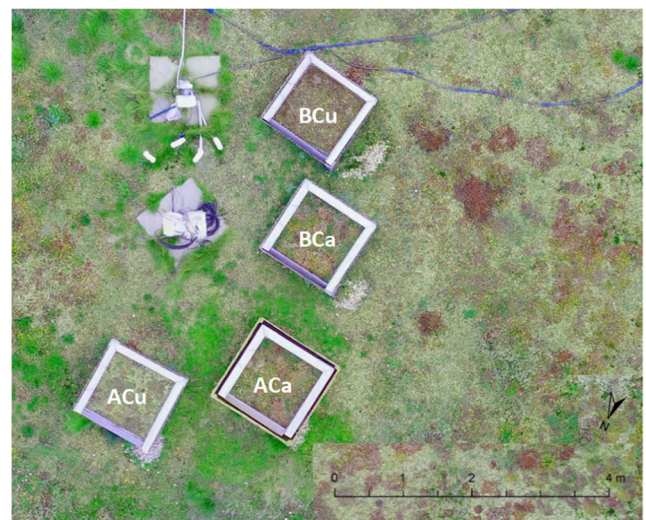

Fig. 2 Aerial view of the experimental site of four extensive green roof test beds

Table 1 Particle size distribution of the two substrates

Particle size range (mm)	Mass fraction	
	A (%)	B (%)
> 2	60.6	67.0
2–0.05	27.1	23.4
0.05–0.002	7.7	5.9
< 0.002	4.6	3.7

### 2.3.2 Retention properties of substrates

The retention curves of the green roof substrates were derived for twelve undisturbed samples taken using sampling rings (5.66 mm in diameter, 4.03 mm high). Three samples were taken from each test bed. Note that samples taken from ACa and BCa contained layers of the sedum carpet at the surface. The retention curves were determined in a sand box (Klute 1986) for matric potentials of 2, 3.5, 10, 33, and 50 cm H_2O and using a water potential meter (WP4C Potential Meter, Decagon Devices, Inc., Pullman, WA) (Kirste et al. 2019), for dry soil. Three saturated salt solutions of potassium carbonate (K_2CO_3), potassium chloride (KCl), and potassium sulfate (K_2SO_4) were used to equilibrate disturbed samples of the substrates in a desiccator with expected relative humidity at 25 °C of 43.16 ± 0.39 %, 84.34 ± 0.26 %, and 97.30 ± 0.45 % respectively (Omega Engineering 2020).

The values measured using the water potential meter ranged from − 165 to − 128 MPa for K_2CO_3 salt; from − 95 to − 33 MPa for KCl; and from − 100 to − 26 MPa for K_2SO_4 salt. The samples were afterwards dried at 60 °C until constant weight to obtain gravimetric water content. The volumetric water content was then obtained as a product of actual mass, humidity, and bulk density. Together with the respective measured water potential values in the soil, these data supplemented the points of the dry end of the retention curve.

Parameters of the retention curves were fitted using the van Genuchten model (van Genuchten 1980) and scaled according to Vogel et al. (1991) using an assumption of linearly variable hydraulic properties to obtain representative retention curves. Representative retention curves of substrates A and B obtained by scaling are shown in Fig. 3.

The parameters of the retention curves are presented in Table 2. Both parameters α and n of the van Genuchten retention curve model were significantly lower than those determined by Palla et al. (2009) for a substrate based on volcanic materials and peat, which suggests a broader grain size distribution in the materials used in this study.

The maximum water holding capacity determined according to the German Landscape Development and Landscaping Research Society guidelines (FLL 2008) was 42.7% for the substrate A and 32.1 % for the substrate B. The dry bulk
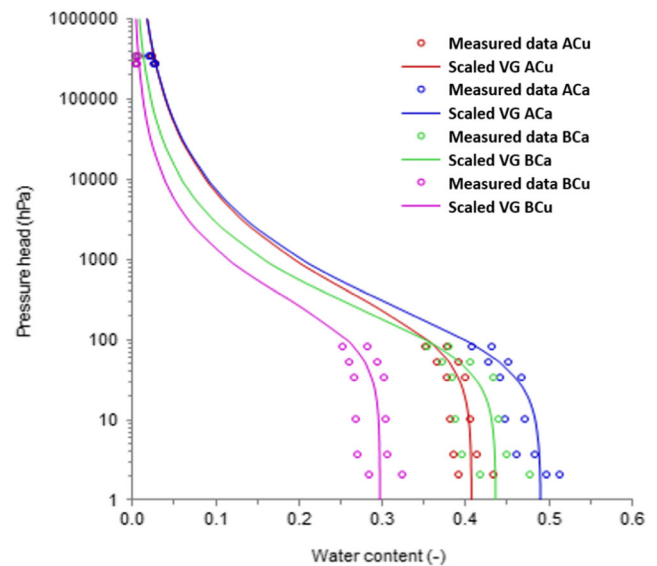
Fig. 3 Measured retention curve points and retention curves obtained by fitting by scaled van Genuchten model for four test beds

density of the substrate A was 890.9 kg m^{-3} whereas for the substrate B it was 475.8 kg m^{-3}. The bulk density of both materials was lower than that of many green roof substrates, e.g., the substrate based on Zeolite reported by Peczkowski et al. (2018) or the substrate based on scoria tuff material used in the study by Conn et al. (2020). The density of the substrates at maximum water capacity was 1318.0 kg m^{-3} for the substrate A and 797.1 kg m^{-3} for the substrate B.

2.3.3 Chemical properties

Selected chemical properties of the leachate from both substrates were determined twice. Disturbed soil samples were taken from each test bed in November 2017 and October 2018 and analyzed in an external laboratory according to the European Committee for Standardization leaching method EN12457-4 (2002) for pH, electrical conductivity, chloride, ammonium, nitrite, nitrates, sulfates, phosphates, COD-Cr—chemical oxygen demand, DOC—dissolved organic carbon, Fe tot, Mn, Ni, Zn, phenol, Cd, Pb, solid TOC—total organic carbon, TN—total nitrogen, and TP—total phosphorus. These parameters were selected as a representative basic screening

Table 2 Measured residual water (θ_r), saturated water content (θ_s), and van Genuchten parameters (α, n)

Test beds	θ_r (cm^3 cm^{-3})	θ_s (cm^3 cm^{-3})	α (cm^{-1})	n (−)
ACu	0	0.407	0.008	1.35
ACa	0	0.490	0.011	1.36
BCu	0	0.297	0.007	1.49
BCa	0	0.436	0.010	1.43

for assessment of leachable nutrients and inorganic contaminants.

Three additional parameters were measured on the solid phase of these same samples. The organic carbon content (TOC) was determined as it is a basic parameter of soil that determines soil sorption and potential for soil structure formation. Total nitrogen (TN) and total phosphorus (TP) were determined as basic nutrients. These parameters were determined in the dried samples; the results are therefore given in milligrams and are based on the weight of the dry matter of the sample.

Characterization of chemical properties was also performed using disturbed samples taken in 2017—immediately after setting up the test beds, and in 2018—after the growing season. Results of the chemical analyses, including pH, conductivity, COD, DOC, basic anions, and basic heavy metals, measured in soil extracts, are presented in table ES 1 in the Electronic supplementary material. The pH results indicate that the substrates were basic, in the 8.0–8.2 range in all test beds. Electrical conductivity (EC) of the substrate B was higher than that in the substrate A. Between 2017 and 2018 EC increased slightly in the ACu, ACa, and BCa test beds, whereas the substrate in the test bed BCu showed a decrease in EC between 2017 and 2018. The initial values of EC were similar to those reported by Aitkenhead-Peterson et al. (2011), who detected a decrease of EC to approximately half of the initial values within six months of operation of green roofs planted with succulents. Similar decreases in the concentrations of chlorides, sulfates, and dissolved organic carbon were seen. Phosphates and total nitrogen increased in BCa unlike the other test beds, where the concentration of phosphates and total nitrogen declined. The observed increase in phosphate in BCa could have been caused by dying and decaying plants (that was observed on that test bed). Nitrite increased during the growing season in all test beds. Nitrates in soil extracts increased significantly for all test beds which is in contrast to the findings of the study of Aitkenhead-Peterson et al. (2011), who observed decline of nitrate concentrations.

Concentration of Fe increased in the leachates between 2017 and 2018. This could be attributable to atmospheric deposition, possibly because the site is located in an industrial area in close proximity to a large steel rolling mill.

Table S1 of the Electronic supplementary material ES 1 also shows that extract from the test beds planted with sedum cuttings had decreased in total phosphorus unlike the extract from the beds planted with sedum carpets where total phosphorus increased—possibly due to translocation of phosphorus from carpet to the substrate underneath it.

2.3.4 Green roof raised beds instrumentation and monitoring

Analysis of the hydrological monitoring was done for the growing season according to the observed meteorological conditions. The growing season is defined for the purposes of this study to have begun the day after the last frost on 04/10/2018 and ended on the first day of snow that occurred on 11/12/2018.

The experimental setup has previously been described in detail by Jelinkova et al. (2015), Jelinkova et al. (2016), and Skala et al. (2019); therefore we will focus mainly on amendments done for the purpose of this study.

The dimensions of each test bed were 1×1 m, with a depth of 0.1 m. The watertight bottom and three sides were made of a 1-mm thick galvanized steel sheet. The test beds were raised approximately 25 cm above the existing green roof of the building in order to allow measurement of the water outflow. The water flowed out of the beds, after passing through all the layers of the green roof into the drainage layer, through a perforated stainless-steel grid on the lowest side of the tray into covered gutters, draining the water directly to tipping bucket flowmeters. The tipping buckets were fitted with electrical heating foil to prevent freezing and damage to the flowmeters. The test beds were isolated from ambient airflow by a 10-cm thick layer of extruded polystyrene located on the sides and under the bottom. The entire structure of each test bed was clad with oriented strand boards.

The tipping bucket flow meters were calibrated by measuring the volume of each bucket. The calibration results indicated one tip per 1.46 mm of rain in test bed ACu, 1.28 mm for ACa, 2.14 mm for BCa, and 2.55 mm for BCu. Outflow from the bed BCa, however, was excluded from the analysis due to unreliable readings obtained from the tipping bucket, an issue that was not resolved for the period of study.

Each test bed was equipped with a temperature probe model 107-L (Campbell Scientific Ltd., Shepshed, UK) which measured the substrate temperature at 1.5 cm above the watertight bottoms of the beds (Fig. 4).

The volumetric water content was measured using eight time domain reflectometry (TDR) probes CS635-L (Campbell Scientific, Inc, Utah, USA) with three 15-cm long rods connected via a multiplexor to a time-domain-reflectometer (TDR 100, Campbell Scientific, Inc, Utah, USA). TDR probes were placed horizontally, with the three rods aligned vertically, two in each test bed approximately 33 cm from the edge and from each other (Fig. 4). Since the composition of green roof substrates differs significantly from natural soils, the commonly used Topp equation (Topp et al. 1980) fails to predict water content from the apparent dielectric constant obtained by TDR. Specific calibrations of measured water content were therefore performed for both substrates. The calibration was done using an approach similar to Kargas et al. (2013). Four samples of each substrate were prepared with defined water content in an aluminum rectangular vessel. The samples were prepared by adding of additional portions of 100 mL of water per 1000 mL of substrate. After adding each dose of water the substrate was well homogenized with a spade. A TDR probe was embedded, and
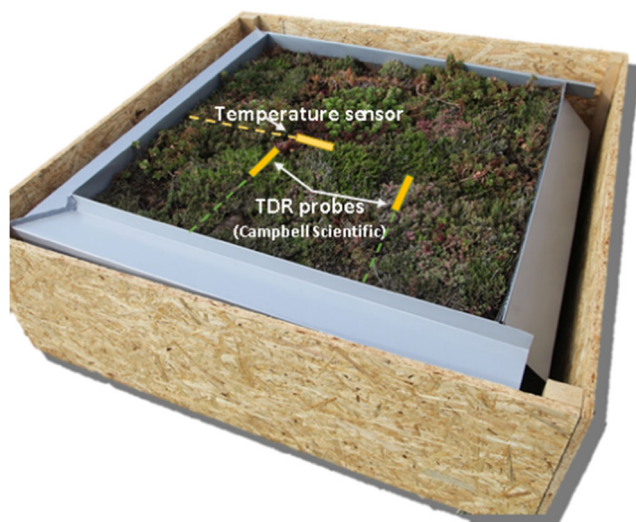
Fig. 4 Schematic plan view of sensor placement in the test bed

the substrate was compacted to a standard bulk density. For the calibration, the minimum water content was set to 0.1 and the maximum was 0.4 (cm^3 cm^{-3}) for both substrates. Apparent dielectric constant was measured each time. The relationship between the actual volumetric water content and apparent dielectric constant was determined as a third-order polynomial using the least square method, and parameters were determined for both substrates.

The green roof layering is shown in Figure 5. Each test bed contained a vegetation layer, a substrate layer, a geotextile filter mat, drainage, and accumulation layer represented by a drainage board, protective geotextile, and a waterproof layer (galvanized steel sheet).

To test the significance of the combined effect of substrate and vegetation cover on substrate temperatures, we ran a one-way analysis of variance (ANOVA). We assumed that thermal behavior of the roof due to solar radiation can be represented by the difference between the maximum air temperature

recorded by a weather station in 200 cm above the roof and the temperature of a substrate of a particular test bed. We tested the null hypothesis stating that the type of green roof does not have impact on the difference between the maximum monthly temperature of the substrate and the maximum monthly air temperature. Additionally, the effect of vegetation on the difference between 75th quartile of monthly temperatures was also tested.

2.3.5 Evaluation of the rainfall-runoff episodes

Runoff coefficients were calculated for each rainfall-runoff episode that occurred during the monitored period. The criteria used to define a rainfall-runoff episode were similar to those used by Jelinkova et al. (2016). A rainfall-runoff episode was defined as having a total rainfall depth greater than 6 mm after the first tip of the rain gauge within the subsequent 6 h. Each rainfall episode was paired with the relevant outflow. Runoff coefficients were calculated as the fraction of the total episode runoff of total episode rainfall.

2.3.6 Vegetation cover monitoring

The vegetation cover was monitored twice a month by photographing each test bed to document changes in the development of the vegetation. The images' perspective was adjusted using the open-source image processing package Fiji ImageJ (Schindelin et al. 2012) to obtain perpendicular pictures. Vegetation cover analysis and image segmentation was performed using the ImageJ WEKA plugin (Arganda-Carreras et al. 2017). The plugin combines a collection of machine learning algorithms with a set of selected image features to produce pixel-based segmentation. The result consisted of two categories, vegetation cover and bare soil. Finally, the proportion of vegetation cover at each time step was calculated from the segmented images.

Fig. 5 Green roof test beds' cross sections describing the layer arrangement of test beds with **a** sedum cuttings and **b** sedum carpet
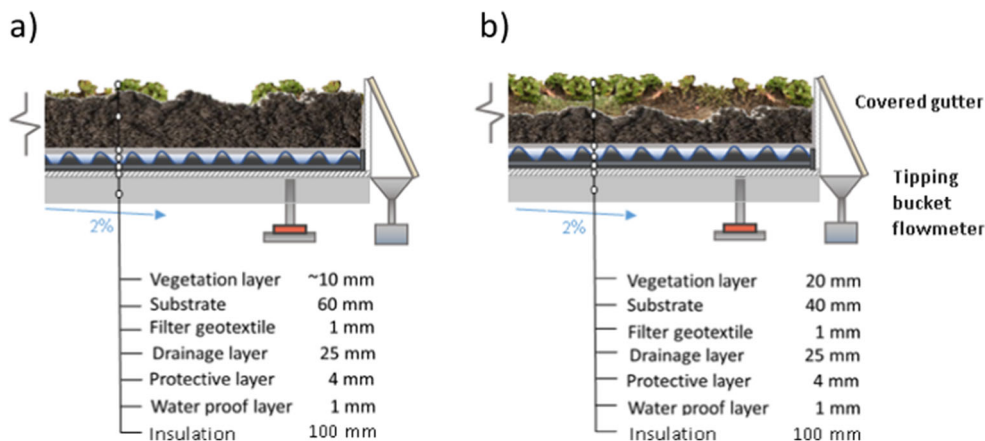
An example of the vegetation cover monitoring and subsequent image processing is shown in Fig. 6. Thanks to fine user-induced tuning, the WEKA algorithm was able to distinguish between substrate and plants. This was especially necessary in distinguishing between the substrate B which has a reddish color and sedum plants that tend to have red-colored leaves in the dormant stage.

3 Results and discussion

Detailed monitoring of green roof raised beds allowed the assessment of water and temperature regimes in the context of different substrates and different plant coverage.

3.1 Green roof raised beds monitoring

3.1.1 Monitoring of water contents and total outflow

Specific TDR probe calibration was performed for both substrates (see Electronic Supplementary Material S4 for calibration curves' shapes). At lower water content, the shapes of the calibration curves were similar for both materials. However, A reached a much higher apparent dielectric constant close to saturation.

In accord with Kargas et al. (2013), we found that the relationship of Ka to θ can be well established for each green roof substrate, but the calibration curve shape is different for each.

Fitting of the relationships between water content and apparent dielectric constant with polynomials produced Eq. 1 for the A substrate and Eq. 2 for the B substrate.
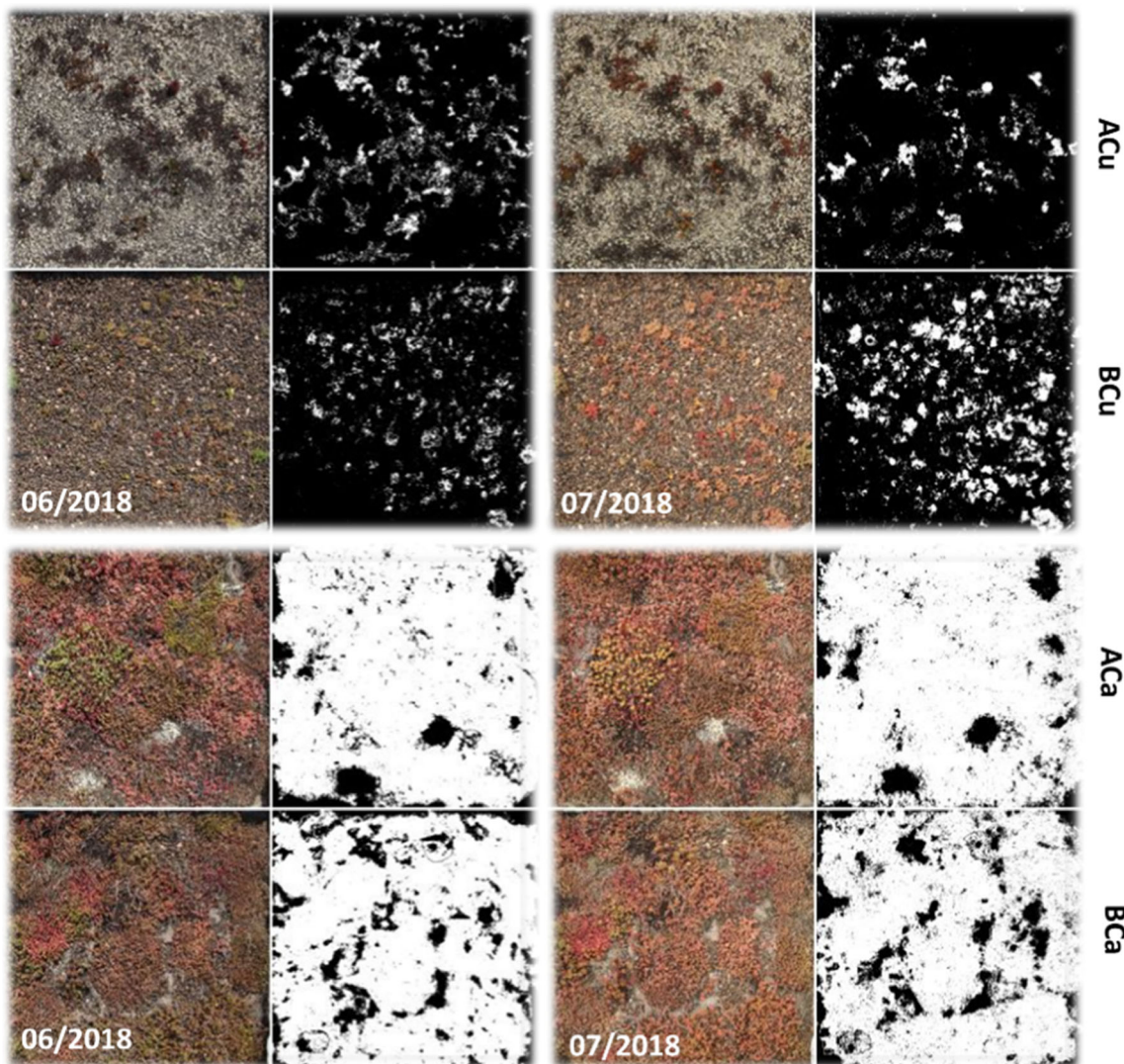

Fig. 6 Example of the vegetation cover determination from the images. Images were taken on June 2018, and July 2018. The color images are the original photographs adjusted for perspective, whereas the black and white images represent the outcome of segmentation, where white color indicates areas covered by plants and black indicates bare surface

$$\theta_A = 0.000285 \times Ka^3 - 0.011433 \times Ka^2 + 0.147257$$
$$\times Ka - 0.208 \tag{1}$$

$$\theta_B = 0.002376 \times Ka^3 - 0.044089 \times Ka^2 + 0.29453$$
$$\times Ka - 0.341 \tag{2}$$

where Ka is the apparent dielectric constant.

Equations 1 and 2 were then used to evaluate volumetric water content for both substrates on the basis of measured apparent dielectric constant. The volumetric water content of the four test beds as indicated by TDR is shown in Fig. 7. We obtained data for each test bed from two TDR probes, with the exception of test bed ACu in which one of the probes produced clearly erroneous values and thus was not included in the data evaluation.

The overall values of water content for ACu and ACa (A) were higher than in BCa and BCu (B). The highest water content as recorded by TDR was consistently observed in ACa. This is in agreement with the measured retention curves, in which ACa exhibited the highest water content over the entire range of water potentials. The highest value of water content was 0.450 cm^3 cm^{-3}, reached in June and August 2018 after several rainfall events, which indicates that the substrate nearly reached full saturation in ACa ($\theta_s = 0.490$ cm cm^{-1}). The water content maxima were higher by 0.15 cm cm^{-1} than those reported by Shafique et al. (2018) from a green roof test bed installed in Seoul, South Korea which was covered by substrate consisting of natural soil (clay, sand, silt, and gravel).

Test bed ACu was generally less saturated, with a peak value at 0.35 cm cm^{-1}. The higher water content maximum in ACa relative to ACu may be attributable to the contribution of the layer of medium on which the sedum carpets were originall grown - mostly based on peat, to the overall water holding capacity of test bed ACa. This theory is supported by the fact that the retention curves of samples from test beds with sedum carpets, i.e., ACa and BCa, had higher saturated water contents than those from the test beds planted with cuttings.

The lowest water content for any rainfall event detected by the TDR sensors was seen in test bed BCa, with a peak value of 0.25 cm cm^{-1} during a rainfall event in June 2018. In the test beds filled with substrate B, test bed BCu (planted with cuttings) reached a higher water content than test bed BCa (planted with carpet). This is the reverse of what was observed in the test beds filled with substrate A. The difference between the two B-filled test beds greater towards the end of the monitoring period in October and November. This observation could not be clearly explained by the data but it may be a result of a capillary barrier effect (Sacha et al. 2019) that would prevent water flow from the finer material (sedum carpet), placed over the significantly coarser material (B substrate). As a result, the water content, measured by the TDR probes, predominantly in the coarse B substrate, was low.

In general, the dynamics of water content variation is characterized by sharp rises caused by rainfall events and slow declines caused by drainage and evapotranspiration. The time of drainage was generally very short, in the order of hours, as can be seen from the cumulative runoff lines in Fig. 7. Evapotranspiration then gradually reduced the water content of the growing media until it reached residual water content. With the absence of rainfall in April, all water storage was depleted in about three weeks in test beds ACa and ACu, whereas in test beds BCu and BCa, storage was depleted in slightly more than a week.

Cumulative runoff from the test beds ACu, ACa, and BCu is shown in Fig. 7. Test bed ACu had the least cumulative runoff (46.1 mm) whereas the highest runoff was observed in BCu (84.3 mm). Slightly less runoff was observed in test bed ACa with a cumulative outflow of 70.4 mm. During the study period, test bed ACu retained 81.5 %, ACa 71.8 %, and
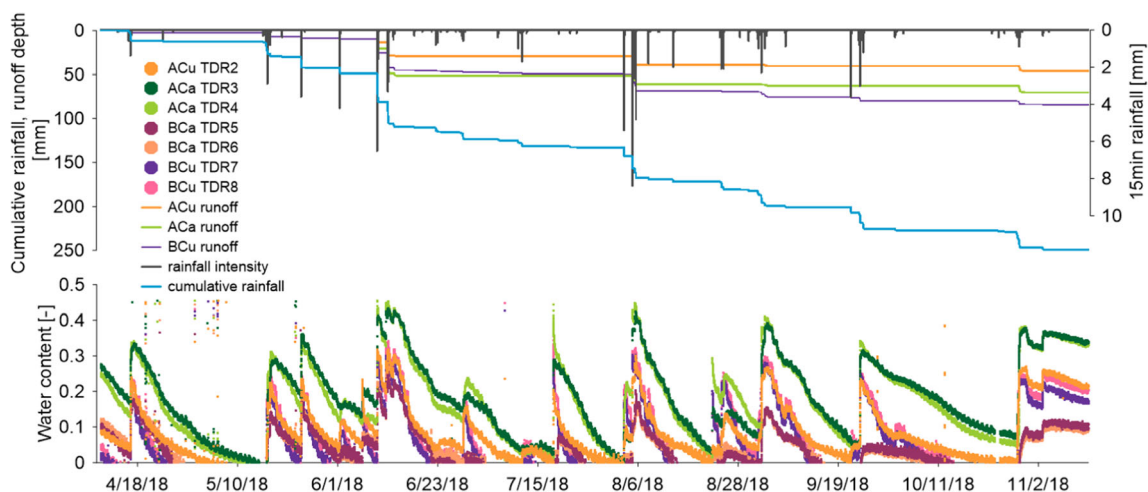

Fig. 7 Volumetric water content and runoff depth of experimental test beds during monitored vegetation season in relation to rainfall

BCu 66.2 % of the total precipitation. The relatively high overall water retention seen (especially for the substrate A) is higher than that reported by Berndtsson et al. (2009) and Stovin et al. (2012), which can be attributed to favorable properties of the substrate, and also to the fact that our observations were made only during the growing season, when substantial evapotranspiration occurs. Inclusion of the winter season, when evapotranspiration is low, would decrease the observed water retention.

3.1.2 Evaluation of rainfall-runoff episodes

In total, thirteen rainfall-runoff episodes were identified. The basic rainfall-runoff characteristics are summarized in Table 3.

The relationship of runoff to rainfall intensity and rainfall amount is illustrated in Figure 8.

Despite there being inadequate number of rainfall-runoff episodes to derive definite rainfall-runoff relationships, the limited season data collected provide some insight into important differences between the different test beds. There were significant differences between runoff from the test beds filled with substrate A and those filled with substrate B. All thirteen rainfall-runoff episodes produced non-zero runoff in the case of BCu, whereas in the case of ACu, only five episodes produced any runoff. Test bed ACa had runoff during only four episodes. Higher runoff coefficients in the case of BCu are undoubtedly the result of the much coarser texture of the B substrate, which allowed water to percolate gravitationally through large pores between the expanded clay, because runoff occurred even during rainfall episodes with rainfall depth less than the retention space of the dry substrate. In general, the runoff coefficients from rainfall episodes with rainfall
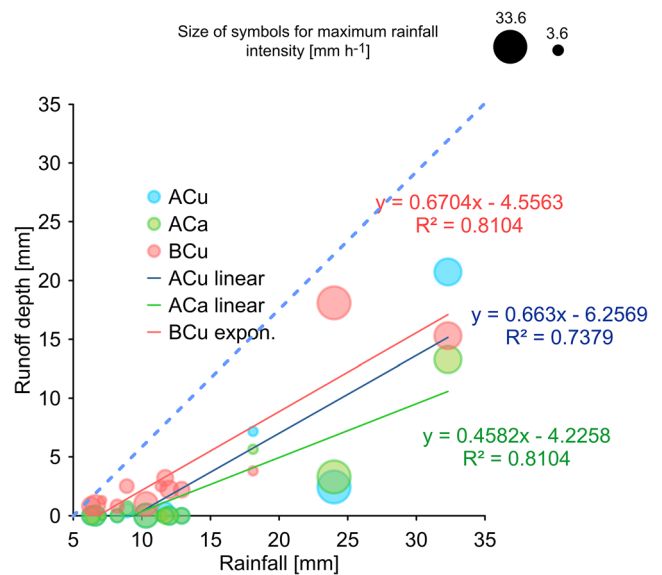

Fig. 8 Rainfall-runoff relationship for test beds ACu, ACa, and BCu

depth below 15 mm were either zero or less than 0.28 (BCu). Three larger rainfall events produced runoff without any clear trend. Rainfall episode no. 5, which had the greatest rainfall amount, led to the highest runoff coefficient in test bed ACu. In the case of the second largest rainfall episode, no. 8, the runoff coefficient of BCu was significantly higher than the runoff coefficient for the other test beds. The source of this inconsistency may be due to the antecedent moisture content of the substrate. Rainfall episode no. 5 started subsequent to several smaller episodes. As ACa normally retained more water and did not deplete its water storage until the beginning of episode no. 5, its free retention space was reduced and

Table 3 Selected rainfall-runoff parameters for 13 rainfall-runoff episodes

Event no.	Initial time	Rainfall depth (mm)	Max rainfall intensity (mm hour^{-1})	Rainfall-runoff episode duration (min)	Runoff coefficient (−)		
					ACu	ACa	BCu
1	16.04.2018 00:00	11.4	5.6	1365	–	–	0.22
2	16.05.2018 02:45	12.9	11.6	1050	–	–	0.17
3	23.05.2018 22:45	12.0	14.4	570	–	–	0.18
4	01.06.2018 11:45	6.6	16.8	540	–	–	0.14
5	09.06.2018 15:15	32.3	26.0	1485	0.64	0.41	0.47
6	28.06.2018 05:15	7.1	2.4	975	–	–	0.18
7	02.08.2018 21:15	10.3	21.6	615	–	–	0.10
8	04.08.2018 19:00	24.0	33.6	435	0.18	0.24	0.75
9	24.08.2018 07:30	8.2	8.4	1230	–	–	0.10
10	02.09.2018 01:30	8.9	9.2	780	0.05	0.07	0.28
11	21.09.2018 18:45	6.3	14.4	570	–	–	0.13
12	23.09.2018 11:15	11.7	12.0	1050	0.04	–	0.27
13	28.10.2018 01:30	18.1	3.6	3330	0.40	0.31	0.21

Fig. 9 **a** Substrate temperature of test beds ACu and ACa. **b** Substrate temperature of test beds BCu and BCa
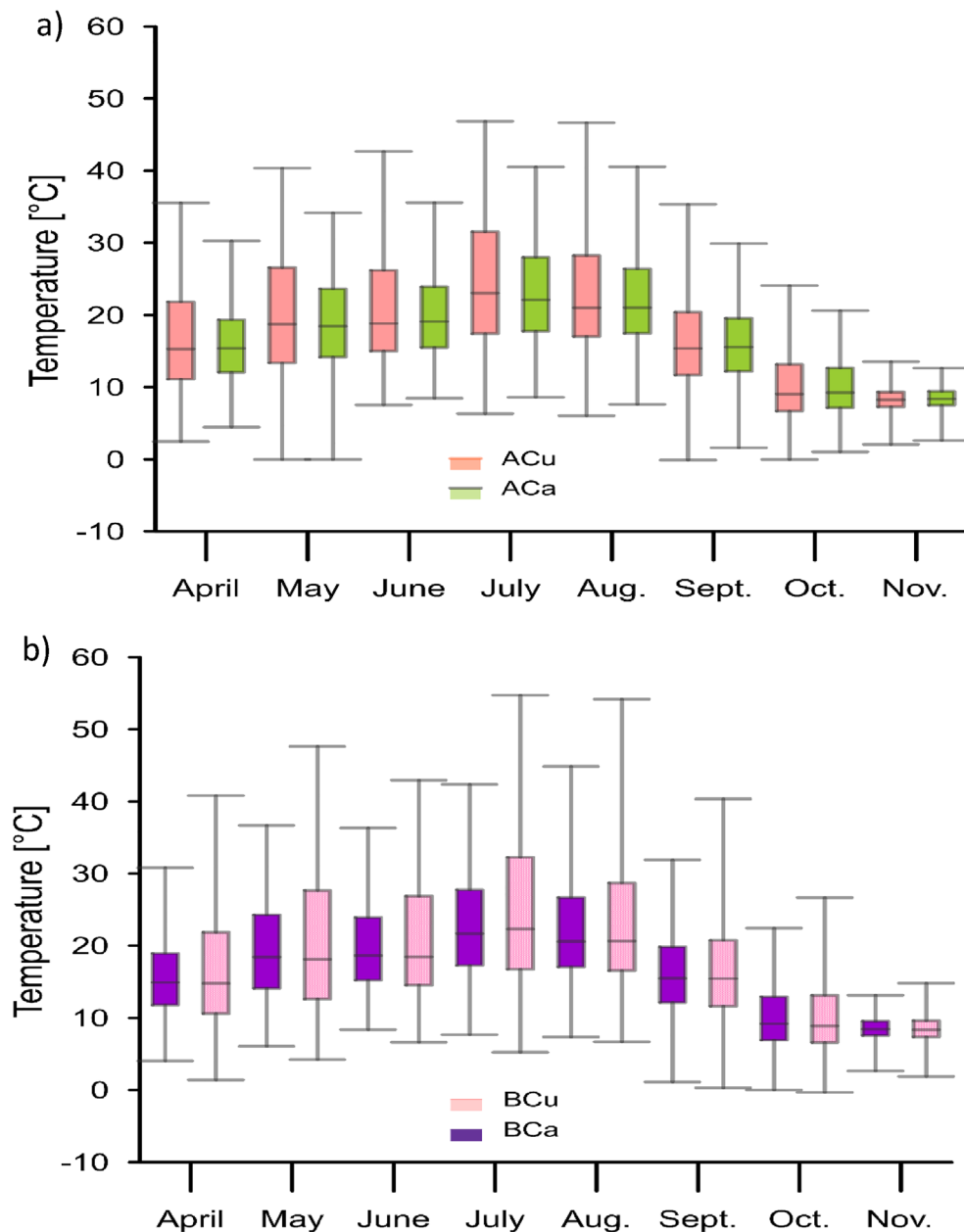
therefore did not retain as much water as other test beds that were dry at the beginning of the event (Fig. 7). In contrast to episode no. 5, the second largest rainfall episode, no. 8, started when the test beds were dry. Therefore the available retention space of each test bed was determined only by its retention capacity, thus BCu retained the least amount of water. Increased antecedent moisture content resulting in decreased retention is logical and well documented, e.g., by Getter et al. (2007). Our observation of reduced retention in test bed ACa emphasizes the importance of having as long as possible a record of antecedent wetting and drying which determines the runoff coefficient from any particular rainfall episode to a significant degree.

3.1.3 Substrate temperatures

The results of substrate temperature monitoring are shown in Fig. 9a for substrate A and Fig. 9b for substrate B. The box plot indicates monthly mean temperatures, the maximum and minimum temperatures in each month, and upper and lower quartiles. In general, the highest maximum temperatures were observed in test bed BCu, which can be explained by higher heat influx from solar radiation through dark bare surfaces between the plants. The maximum substrate temperatures in test bed ACu were significantly lower, despite the surface between the plants being equally exposed to solar radiation. The albedo of the substrate A is higher due to the very light
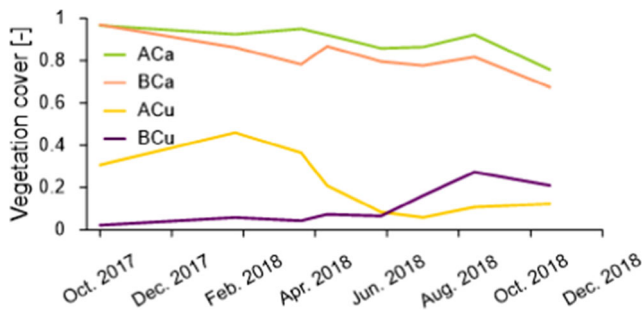
Fig. 10 The development of the vegetation cover on four test beds

color of spongolite. Our observation that darker, more exposed substrate results in higher temperatures is in accordance with the early study of Oke and Hannell (1966) and with the findings of the recent study by Kodesova et al. (2014) who found that darker, bare surface of Technosol led to higher maximum temperatures compared to lighter colored substrates or vegetated surfaces.

Greater vegetation coverage led to significantly lower maximum substrate temperatures in both A and B. The temperatures of the substrates were nearly the same in all test beds in September, October, and November, when the effects of insolation and vegetative cover were minimal.

According to result of ANOVA, the type of green roof (characterized by planting style and substrate) had a significant impact on the difference between the monthly maximum temperature of substrate and maximum monthly air temperature, $F_{(3,28)} = 5.16$, $p = 0.0058$ for the entire growing season, whereas the significance was even higher for the months of April–August, $F_{(3,12)} = 36.7$, $p = 2.5 \times 10^{-6}$. The type of green roof had a significant impact on the difference between 75th quartile of monthly substrate temperature and 75th quartile of monthly air temperatures for the months of April–August, $F_{(3,16)} = 6.17$, $p = 0.0055$, but not significant for all months of the growing season taken together $F_{(3,28)} = 2.173$, $p = 0.11$.

3.1.4 Vegetation cover monitoring

Vegetation growth in the test beds after planting is presented in Fig. 10 for the period between planting in October 2017 until the end of the 2018 growing season. The test beds covered with sedum carpets, test beds ACa and BCa, displayed a decrease in vegetation coverage of 15–20% between October 2017 and July 2018. In the other two test beds, planted with individual rooted pieces of sedum cuttings, vegetation cover of ACu spread widely in November 2017, but declined over the winter prior to the experimental period, and vegetation cover of test bed BCu remained nearly unchanged until June 2018 and only then started to increase.

4 Conclusions

The spongolite-based (A) and expanded clay-based (B) substrate test beds—planted with pre-prepared sedum carpet—retained more water than did those planted with sedum cuttings. Therefore, if flattening and delaying the peak runoff is the primary consideration in a green roof installation, then the use of pre-prepared carpets of sedum in preference to using cuttings is highly recommended. However the plant coverage declined in the case of sedum carpets, while the coverage increased in the case of cuttings during the first year of operation; therefore, it can be expected that the advantage of sedum carpets will last only for the first few growing seasons assuming that this trend would continue until coverage was comparable.

There were a limited number of rainfall episodes during the study period, making definitive conclusions about rainfall-runoff characteristics for the substrates difficult; however, it is clear that the beds containing the coarser substrate, B, had more outflow. Once again, if delaying peak runoff is a key priority at an installation, finer substrates, which perform better in this regard, should be employed.

Regarding the thermal regulating ability of green roofs, our results clearly indicate that beds planted with sedum carpets, and having more extensive vegetation coverage, were superior at moderating extremes of temperature.

Thus, in regard to both water retention/runoff peak delay and thermal regulation, it is clear from our observations that the denser vegetation coverage afforded by the sedum carpets, in contrast to the sedum cuttings, results in better control of both factors.

The monitoring of the experimental installation continues and will produce data for numerical model validation. Promising approaches to modeling water regimes in green roof layers have recently been outlined, e.g., by Skala et al. (2019, 2020).

Data availability The data presented in this publication can be provided on request.

Compliance with ethical standards

Conflict of interest The authors declare that they have no conflict of interest.

Research involving human participants and/or animals and informed consent Not applicable.

References

Aitkenhead-Peterson JA, Dvorak BD, Voider A, Stanley NC (2011) Chemistry of growth medium and leachate from green roof systems in south-central Texas. Urban Ecosyst 14:17–33. https://doi.org/10.1007/s11252-010-0137-4

Akther M, He JX, Chu A, van Duin B (2020) Chemical leaching behaviour of a full-scale green roof in a cold and semi-arid climate. Ecol Eng 147:105768. https://doi.org/10.1016/j.ecoleng.2020.105768

Arganda-Carreras I, Kaynig V, Rueden C, Eliceiri KW, Schindelin J, Cardona A, Seung HS (2017) Trainable Weka Segmentation: a machine learning tool for microscopy pixel classification. Bioinformatics 33:2424–2426. https://doi.org/10.1093/bioinformatics/btx180

Beecham S, Razzaghmanesh M (2015) Water quality and quantity investigation of green roofs in a dry climate. Water Res 70:370–384. https://doi.org/10.1016/j.watres.2014.12.015

Bengtsson L, Grahn L, Olsson J (2005) Hydrological function of a thin extensive green roof in southern Sweden. Hydrol Res 36:259–268. https://doi.org/10.2166/nh.2005.0019

Berndtsson JC, Bengtsson L, Jinno K (2009) Runoff water quality from intensive and extensive vegetated roofs. Ecol Eng 35:369–380. https://doi.org/10.1016/j.ecoleng.2008.09.020

Berretta C, Poë S, Stovin V (2014) The influence of growing media and vegetation on extensive green roof hydrological performance. In: 13th International Conference on Urban Drainage. ICID 2014, 07-12 Sep 2014, Malaysia.

Bevilacqua P, Mazzeo D, Bruno R, Arcuri N (2016) Experimental investigation of the thermal performances of an extensive green roof in the Mediterranean area. Energy and Build 122:63–79. https://doi.org/10.1016/j.enbuild.2016.03.062

Bouzouidja R, Béchet B, Hanzlikova J, Sněhota M, Le Guern C, Capiaux H, Jean-Soro L, Claverie R, Jomiel S, Schwartz C, Guénon R, Szkordilisz F, Musy M, Körmöndi B, Cannavo P, Lebeau T (2020) Simplified performance assessment methodology for addressing soil quality of nature-based-solutions. J Soils Sediments. https://doi.org/10.1007/s11368-020-02731-y

Brandao C, Cameira MR, Valente F, de Carvalho RC, Paco TA (2017) Wet season hydrological performance of green roofs using native species under Mediterranean climate. Ecol Eng 102:596–611. https://doi.org/10.1016/j.ecoleng.2017.02.025

Casagrande A (1934) Die Aräometer-Methode zur Bestimmung der Kornverteilung von Böden und anderen Materialien (in German). Julius Springer, Berlin

Conn R, Werdin J, Rayner JP, Farrell C (2020) Green roof substrate physical properties differ between standard laboratory tests due to differences in compaction. J Environ Manage 261:110206. https://doi.org/10.1016/j.jenvman.2020.110206

da Silva M, Najjar MK, Hammad AWA, Haddad A, Vazquez E (2020) Assessing the retention capacity of an experimental green roof prototype. Water 12:90. https://doi.org/10.3390/w12010090

EN 12457-4 (2002) Characterisation of waste leaching compliance test for leaching of granular waste materials and sludges - part 4: one-stage batch test at a liquid to solids ratio of 10 L/kg for materials with a particle size below 10 mm (with or without size reduction), CEN/TC292/WG2, European Committee for Standardization, Brussels

FLL (2008) Guidelines for the planning, construction and maintenance of green roofing. Forschungsgesellschaft Landschaftsentwicklung Landschaftsbau e.V, Bonn, Germany

Getter KL, Rowe DB, Andresen JA (2007) Quantifying the effect of slope on extensive green roof stormwater retention. Ecol Eng 31:225–231. https://doi.org/10.1016/j.ecoleng.2007.06.004

Gong YW, Yin DK, Li JQ, Zhang XW, Wang WH, Fang X, Shi HH, Wang Q (2019) Performance assessment of extensive green roof runoff flow and quality control capacity based on pilot experiments. Sci Tot Environ 687:505–515. https://doi.org/10.1016/j.scitotenv.2019.06.100

Jelinkova V, Dohnal M, Picek T (2015) A green roof segment for monitoring the hydrological and thermal behaviour of anthropogenic soil systems. Soil Water Res 10:262–270. https://doi.org/10.17221/17/2015-SWR

Jelinkova V, Dohnal M, Sacha J (2016) Thermal and water regime studied in a thin soil layer of green roof systems at early stage of pedogenesis. J Soils Sediments 16:2568–2579. https://doi.org/10.1007/s11368-016-1457-7

Kargas G, Ntoulas N, Nektarios PA (2013) Moisture content measurements of green roof substrates using two dielectric sensors. Hort Technology 23:177–186. https://doi.org/10.21273/HORTTECH.23.2.177

Kirste B, Iden SC, Durner W (2019) Determination of the soil water retention curve around the wilting point: optimized protocol for the dewpoint method. Soil Sci Soc Am J 83:288–299. https://doi.org/10.2136/sssaj2018.08.0286

Klute A (1986) Water retention: Laboratory methods. In: A. Klute (ed.) Methods of soil analysis. Part 1. Physical and mineralogical methods. American Society of Agronomy-Soil Science Society of America, Madison, Wisconsin, 635-662.

Kodesova R, Fer M, Klement A, Nikodem A, Tepla D, Neuberger P, Bures P (2014) Impact of various surface covers on water and thermal regime of Technosol. J Hydrol 51:2272–2288. https://doi.org/10.1016/j.jhydrol.2014.10.035

Lehmann S (2014) Low carbon districts: mitigating the urban heat island with green roof infrastructure. City Cult Soc 5:1–8. https://doi.org/10.1016/j.ccs.2014.02.002

Li XX, Cao JJ, Xu PX, Fei L, Dong Q, Wang ZL (2018) Green roofs: effects of plant species used on runoff. Land Degrad Dev 29:3628–3638. https://doi.org/10.1002/ldr.3102

Mentens J, Raes D, Hermy M (2006) Green roofs as a tool for solving the rainwater runoff problem in the urbanized 21st century? Landscape Urban Plan 77:217–226. https://doi.org/10.1016/j.landurbplan.2005.02.010

Oke TR, Hannell FG (1966) Variation of temperatures within a soil. Weather 21:21–28. https://doi.org/10.1002/j.1477-8696.1966.tb05184.x

Omega Engineering: Equilibrium relative humidity saturated salt solutions. https://www.omega.com/temperature/z/pdf/z103.pdf. Accessed August 1, 2020.

Palla A, Gnecco I, Lanza LG (2009) Unsaturated 2D modelling of subsurface water flow in the coarse-grained porous matrix of a green roof. J Hydrol 379:193–204. https://doi.org/10.1016/j.jhydrol.2009.10.008

Peczkowski G, Kowalczyk T, Szawernoga K, Orzepowski W, Zmuda R, Pokladek R (2018) Hydrological performance and runoff water quality of experimental green roofs. Water 10:15. https://doi.org/10.3390/w10091185

Robine JM, Cheung SLK, Le Roy S, Van Oyen H, Griffiths C, Michel JP, Herrmann FR (2008) Death toll exceeded 70,000 in Europe during the summer of 2003. C R Biol 331:171–178. https://doi.org/10.1016/j.crvi.2007.12.001

Sacha J, Snehota M, Trtik P, Hovind J (2019) Impact of infiltration rate on residual air distribution and hydraulic conductivity. Vadose Zone J 18:1–15. https://doi.org/10.2136/vzj2019.01.0003

Schindelin J, Arganda-Carreras I, Frise E (2012) Fiji: an open-source platform for biological-image analysis. Nat Methods 9:676–682. https://doi.org/10.1038/nmeth.2019

Schroll E, Lambrinos J, Righetti T, Sandrock D (2011) The role of vegetation in regulating stormwater runoff from green roofs in a winter rainfall climate. Ecol Eng 37:595–600. https://doi.org/10.1016/j.ecoleng.2010.12.020

Shafique M, Kim R, Kyung-Ho K (2018) Green roof for stormwater management in a highly urbanized area: the case of Seoul, Korea. Sustainability 10. https://doi.org/10.3390/su10030584

Skala V, Dohnal M, Votrubova J, Jelinkova V (2019) The use of simple hydrological models to assess outflow of two green roofs systems. Soil and Water Res 14:94–103. https://doi.org/10.17221/138/2018-SWR

Skala V, Dohnal M, Votrubova J, Vogel T, Dusek, J, Sacha J, Jelinkova V (2020) Hydrological and thermal regime of a thin green roof system evaluated by physically-based model. Urban For Urban Gree 48. https://doi.org/10.1016/j.ufug.2020.126582

Speak AF, Rothwell JJ, Lindley SJ, Smith CL (2013) Rainwater runoff retention on an aged intensive green roof. Sci Total Environ 461-462:28–38. https://doi.org/10.1016/j.scitotenv.2013.04.085

Stovin V (2010) The potential of green roofs to manage urban stormwater. Water Environ J 24:192–199. https://doi.org/10.1111/j.1747-6593.2009.00174.x

Stovin V, Vesuviano G, Kasmin H (2012) The hydrological performance of a green roof test bed under UK climatic conditions. J Hydrol 414:148–161. https://doi.org/10.1016/j.jhydrol.2011.10.022

Topp GC, Davis JL, Annan AP (1980) Electromagnetic determination of soil water content: Measurements in coaxial transmission lines. Water Resour Res 16:574–582. https://doi.org/10.1029/WR016i003p00574

van Genuchten MT (1980) A closed-form equation for predicting the hydraulic conductivity of unsaturated soils. Sci Soc Am J 44:892–898. https://doi.org/10.2136/sssaj1980.03615995004400050002x

VanWoert N, Rowe D, Andresen J, Rugh C, Fernandez R, Xiao L (2005) Green roof stormwater retention: effects of roof surface, slope, and media depth. J Environ Qual 34:1036–1044. https://doi.org/10.2134/jeq2004.0364

Versini PA, Stanic F, Gires A, Schertzer D, Tchiguirinskaia I (2020) Measurements of the water balance components of a large green roof in the greater Paris area. Earth Syst Sci Data 12:1025–1035. https://doi.org/10.5194/essd-12-1025-2020

Vogel T, Císlerová M, Hopmans JW (1991) Porous-media with linearly variable hydraulic properties. Water Resour Res 27:2735–2741. https://doi.org/10.1029/91WR01676

Voyde E, Fassman E, Simcock R (2010) Hydrology of an extensive living roof under sub-tropical climate conditions in Auckland, New Zealand. J Hydrol 394:384–395. https://doi.org/10.1016/j.jhydrol.2010.09.013

Wang X, Tian Y, Zhao X (2017) The influence of dual-substrate-layer extensive green roofs on rainwater runoff quantity and quality. Sci Total Environ 592:465–476. https://doi.org/10.1016/j.scitotenv.2017.03.124